Synthesis of Triamine on OMS-2 Support for Removal of Nitrate and Phosphate in Water

Trung Thanh Nguyen[1,2], Tri Thich Le[1,2], Tuan Cuong Trinh[2,3], Le Ba Tran[1,2,4,5], Phuoc Toan Phan[1,2,4,5], Thuy Nguyen Thi[2,6], Surapol Padungthon[7], Nhat Huy Nguyen[2,5]*

[1]Laboratory of Nanomaterial, An Giang University, 18 Ung Van Khiem St., Dong Xuyen Dist., Long Xuyen City, An Giang Province, Vietnam

[2]Vietnam National University Ho Chi Minh City, Linh Trung Ward, Thu Duc City, Ho Chi Minh City, Vietnam

[3]Institute for Environment and Resources, 142 To Hien Thanh St., Dist. 10, Ho Chi Minh City, Vietnam

[4]Faculty of Engineering - Technology - Environment, An Giang University, 18 Ung Van Khiem St., Dong Xuyen Dist., Long Xuyen City, An Giang Province, Vietnam

[5]Faculty of Environment and Natural Resources, Ho Chi Minh City University of Technology (HCMUT), 268 Ly Thuong Kiet St., Dist. 10, Ho Chi Minh City, Vietnam

[6]School of Chemical and Environmental Engineering, International University, Quarter 6, Linh Trung Ward, Thu Duc City, Ho Chi Minh City, Vietnam

[7]Department of Environmental Engineering, Khon Kaen University, 123 Moo 16 Mittraphap Rd., Nai-Muang, Muang District, Khon Kaen 40002, Thailand

*Corresponding author (e-mail: nnhuy@hcmut.edu.vn)

The combination of amine groups and an OMS-2 carrier matrix resulted in a new material (Amine-OMS-2) that could be used for the effective adsorption of nitrate and phosphate ions in water. This material was then characterized by SEM, XRD, FTIR, TGA, and BET. In nitrate and phosphate adsorption tests, Amine-OMS-2 reached adsorption equilibrium after 30 and 60 min, respectively. Adsorption using Amine-OMS-2 followed an apparent second-order kinetic model with maximum adsorption capacities of 34.1 mg g^{-1} (pH 5, nitrate) and 12.2 mg g^{-1} (pH 6, phosphate). Adsorption capacity was proportional to initial anion concentration and inversely proportional to temperature. In the treatment of real wastewater, Amine-OMS-2 was found to be a multi-purpose adsorbent for removing nitrate, phosphate and organics simultaneously, with high adsorption capacities of 11.1 mg g^{-1}, 16.8 mg g^{-1}, and 22.4 mg COD L^{-1}. These results demonstrate the ability of Amine-OMS-2 to remove excess nutrients and organic components in wastewater.

Keywords: Amine grafting; nitrate; phosphate; adsorption; OMS-2

Received: September 2022; Accepted: July 2023

Nitrate and phosphate pollution is dangerous to the environment. They arise from untreated or improperly treated urban and industrial wastewater, as well as from the overuse of fertilizers in agricultural activities. Once these nutrients are released into the environment, they cause pollution, such as eutrophication, which reduces the oxygen content of water, and causes harm to aquatic organisms [1]. In the human body, nitrate can be converted into toxic nitrite and combined with haemoglobin to form methaemoglobin, which poisons the body and causes death in babies [2, 3]. Besides this, nitrite can react with other amino acids in the body to form nitrosamine, a potentially carcinogenic compound [4]. Similarly, being exposed to large doses of phosphate over 1–7 years increases the occurrence of soft tissue calcification and impairs kidney function, leading to calcium and phosphate clumping in the blood, bones, joints, blood and blood vessels, causing joint pain or fractures [5]. Therefore, removing nitrate and phosphate from wastewater is necessary before it is discharged into the environment.

Currently, there are several widely applied technologies for nitrate and phosphate treatment, such as activated sludge [6], constructed wetlands [7], ion exchange [8], reverse osmosis [9], chemical precipitation [10], membrane [11, 12] and adsorption [13]. Among them, the conventional anaerobic-anoxic-oxic technology is widely used in practical applications. However, there are still some limitations, such as a high pollutant concentration requirement, the existence of these pollutants even after the biological treatment process, complicated operation, and removal efficiency affected by temperature, sludge condition, volatile fatty acids and pH [14]. Recently, adsorption emerged as a simple and effective water and wastewater treatment with stable operation and less sludge production. Therefore, adsorption could be applied as an add-on to traditional biological processes for removing nitrate and phosphate in small and medium enterprises with low nitrate and phosphate concentrations. For this purpose, various adsorbents have been prepared and examined for the removal

of phosphate and nitrate, including amine-chitosan [15], MgO-biochar [16], certain chitosans [17], amine-SiO_2 [18, 19], anion exchange resin-supported iron hydroxide [20], amine grafted activated rice husk ash [21, 22], amine grafted on iron oxides/hydroxides [23], Mg- and Fe-supported cation exchange resins [24], and flower-like iron oxide on activated rice husk ash [25]. Recently, an octahedral molecular sieve (OMS-2) has attracted much attention [26]. However, there are very limited reports on the synthesis and application of amine-grafted OMS-2 for simultaneously removing nitrate, phosphate and organic pollutants in wastewater.

In this work, we aim to prepare a new material, an amine-grafted OMS-2, and apply it as an adsorbent for removing nitrate, phosphate and organic pollutants in both synthetic and real wastewater. In the batch adsorption test, the effect of environmental conditions (e.g., temperature, solution pH, initial nitrate and phosphate concentrations and adsorbent dosage) were investigated. The kinetics and isotherms of the nitrate and phosphate adsorption reactions using the synthesized material were also examined.

EXPERIMENTAL

Chemicals and Materials

Chemicals used were lab-grade, such as KNO_3, $KMnO_4$, $K_2Cr_2O_7$, $C_6H_6O_6$, KH_2PO_4, NaOH, ascorbic acid, HNO_3, $FeCl_3.6H_2O$, $MnSO_4.H_2O$, NH_4Cl, toluene, sulfanilamide, $C_4H_4KNaO_6.4H_2O$ with a purity of ≥ 99.5 %. H_2SO_4 (98 %), HCl (36 %), $HgSO_4$ (99 %), and N-(1-naphthyl)-ethylenediamine dihydrochloride (99.5 %) were purchased from Xilong Scientific (China). NaOH, ascorbic acid, KBr, and $K(SbO)C_4H_4O_8.1/2H_2O$ with a purity of 99.5% were obtained from Merck, Germany. N^1-(3-Trimethoxysilylpropyl)diethylenetriamine (technical grade) was sourced from Sigma Aldrich (USA). Deionized distilled water was used for material synthesis, preparation of nitrate and phosphate wastewater, and analytical and experimental operations.

The OMS-2 support was synthesized following a procedure reported previously [27-29]. The grafting of amine on the OMS-2 material was carried out based on a literature method, using an OMS-2 support instead of iron oxide, silica, or activated rice husk ash [19, 22, 23].

Characterization Methods

Surface chemical properties were determined by Fourier-transform infrared spectroscopy (FTIR, Alpha, Bruker, Germany). Morphology was examined by scanning electron microscopy (SEM) coupled with energy dispersive X-ray analysis (EDX) (SEM-EDX, JCM-7000, JEOL, Japan). The thermal stability of the material was studied by thermogravimetric analysis (TGA, Q500, TA Instruments, USA). The crystalline structure of the material was characterized by X-ray powder diffraction (XRD, AERIS, Malvern Panalytical, Netherlands). The surface area of the material was measured by the N_2 adsorption-desorption method (BET, BET-202A, Porous Materials, USA). The point of zero charge (pHpzc) of the Amine-OMS-2 material was determined by a titration method using KCl solution, and the solution pH was adjusted by adding HCl or NaOH solution [30]. The concentrations of nitrate and phosphate in the solution before and after adsorption were analysed by UV–Vis spectroscopy (SPECORD 210, Analytik Jena, Germany).

Adsorption Tests

Batch nitrate and phosphate adsorption experiments were conducted to determine optimal adsorption conditions. The adsorption tests were done under the same conditions, with a material weight of 30 mg and a 50 mL solution containing nitrate (50 mg L^{-1}) and/or phosphate (10 mg L^{-1}). Effects of the operational parameters on nitrate and phosphate adsorption were investigated under different pH conditions (2-11), material mass (5-100 mg), adsorption time (0-120 min), initial concentration (10-500 and 2-120 mg L^{-1} for nitrate and phosphate, respectively), and temperature (20-40 ^oC). All the adsorption experiments for water, as well as blank samples, were conducted on 3 replicates and the averaged results are presented in this work. The nitrate concentration was determined according to TCVN 4562:1988 (Vietnam standard: Wastewater – Method of determining nitrate content), and the phosphate concentration was determined according to TCVN 6202:2008 (Vietnam standard: Water quality – Determination of phosphorus – Spectrometric method using ammonium molybdate).

The nitrate and phosphate adsorption capacities of the material were evaluated with Eq. 1,

$$q_e = \frac{C_0 - C_e}{m} \times V \qquad \text{(Eq. 1)}$$

where q_e is the nitrate or phosphate adsorption capacity (mg g^{-1}), C_0 and C_e are the initial and equilibrium concentrations of nitrate or phosphate (mg L^{-1}), V is the solution volume (L), and m is the mass of Amine-OMS-2 (g).

RESULTS AND DISCUSSION

Characterization of materials

Amine-OMS-2 was prepared by attaching triamine groups to the OMS-2 surface based on the reaction between triamine silane and OMS-2. After amine grafting, the material had a grey-black colour which was lighter than the original OMS-2. The specific surface area of the Amine-OMS-2 material was determined by the BET method to be 8.35 m^2 g^{-1}, which was much lower than that of the original OMS-2 (~ 57.62 m^2 g^{-1}), possibly due to the coating of amines around the OMS-2 surface and in its pore structure.

The chemical structures on the surface of Amine-OMS-2 before and after adsorption were determined by FTIR. As observed in Fig. 1, OMS-2 with its octahedral structure was clearly indicated by the peaks at 700 to 400 cm^{-1} [31], in which the vibration around 469 cm^{-1} was characteristic of Mn^{2+} in the material structure [32], while 581 and 709 cm^{-1} were ascribed to vibrations of the OMS-2 octahedral framework [33]. The analysis showed that all three materials had peaks at 3452 cm^{-1}, which was the characteristic vibration of the H-O-H bond in H_2O molecules [34]. The peaks between 3480 and 3508 cm^{-1} in amine-containing materials are due to the vibrations of the -NH group and the O-H group of water adsorbed on the material [15]. After amine impregnation, the sample exhibited the characteristic peak of the N-H bond at 1626 cm^{-1} [35] and the stretching vibration of the amine group at 1480 cm^{-1} [36]. After adsorption of nitrate and phosphate, there were peaks at 1384 cm^{-1} for nitrate [37] and 908 cm^{-1} for phosphate [38], proving the effective adsorption ability of Amine-OMS-2.

Fig. 2 displays the XRD patterns of OMS-2 and Amine-OMS-2. For OMS-2, the peaks at 2θ of 12.4, 17.7, 29.1, 37.6, 42.2, 50.0 and 60.4° correspond to the (110), (200), (310), (211), (301), (411), and (521) planes, respectively, [39] consistent with cryptomylane (KMn_8O_{16}) [34]. This crystalline structure was retained after amine grafting (i.e. in Amine-OMS-2), proving that this procedure did not affect the crystallinity of the material. The particle sizes (d) were then calculated using the Debye–Scherrer equation (Eq. 2),

$$d = \frac{K\lambda}{\beta \cos\theta} \qquad \text{(Eq. 2)}$$

where k = 0.9 is the Debye–Scherrer constant, λ = 0.15406 nm is the X-ray wavelength, β is the full width at half maximum, and θ is the Bragg angle.

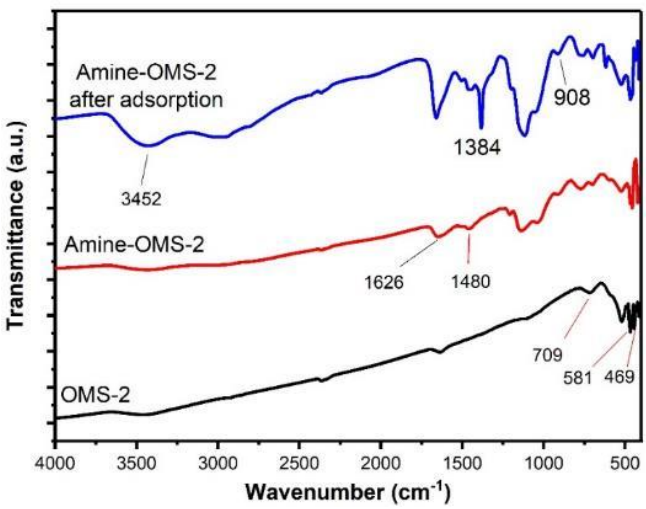

Figure 1. FTIR spectra of OMS-2 and Amine-OMS-2.

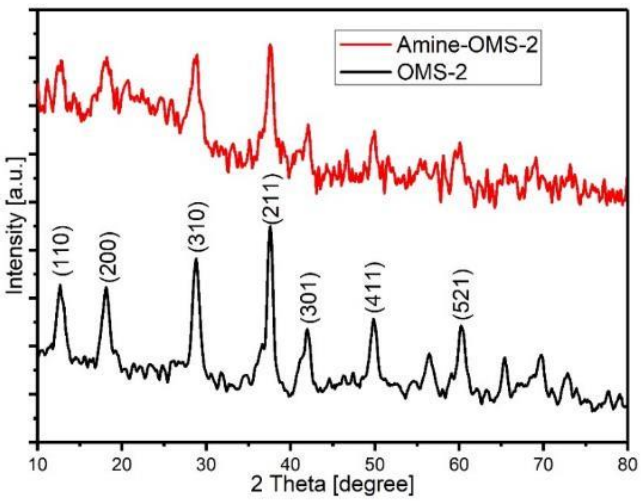

Figure 2. XRD patterns of OMS-2 and Amine-OMS-2.

The average particle sizes of OMS-2 and Amine-OMS-2, calculated at 2θ of 37.6°, were 9.64 nm and 8.21 nm, respectively. The insignificant difference between the particle sizes of OMS-2 and Amine-OMS-2 may be due to the small amount of amine grafted onto the OMS-2 support.

As seen in Fig. 3 (a) and (b), the OMS-2 support had a three-dimensional rod-like shape with the MnO_6 octahedral as the main structure forming a porous framework material. Fig. 3 (c) and (d) show that the surface of the particles became smoother after amine grafting, which was the cause of the decrease in specific surface area for Amine OMS-2 in the BET results. The EDX and EDX-mapping results of Amine-OMS-2 are displayed in Fig. 3 (e). Four elements were uniformly dispersed on the OMS-2 surface with a weight percentage of C (44.40%) > O (35.92%) > N (17.60%) > Si (2.07%), similar to the grafted amine component.

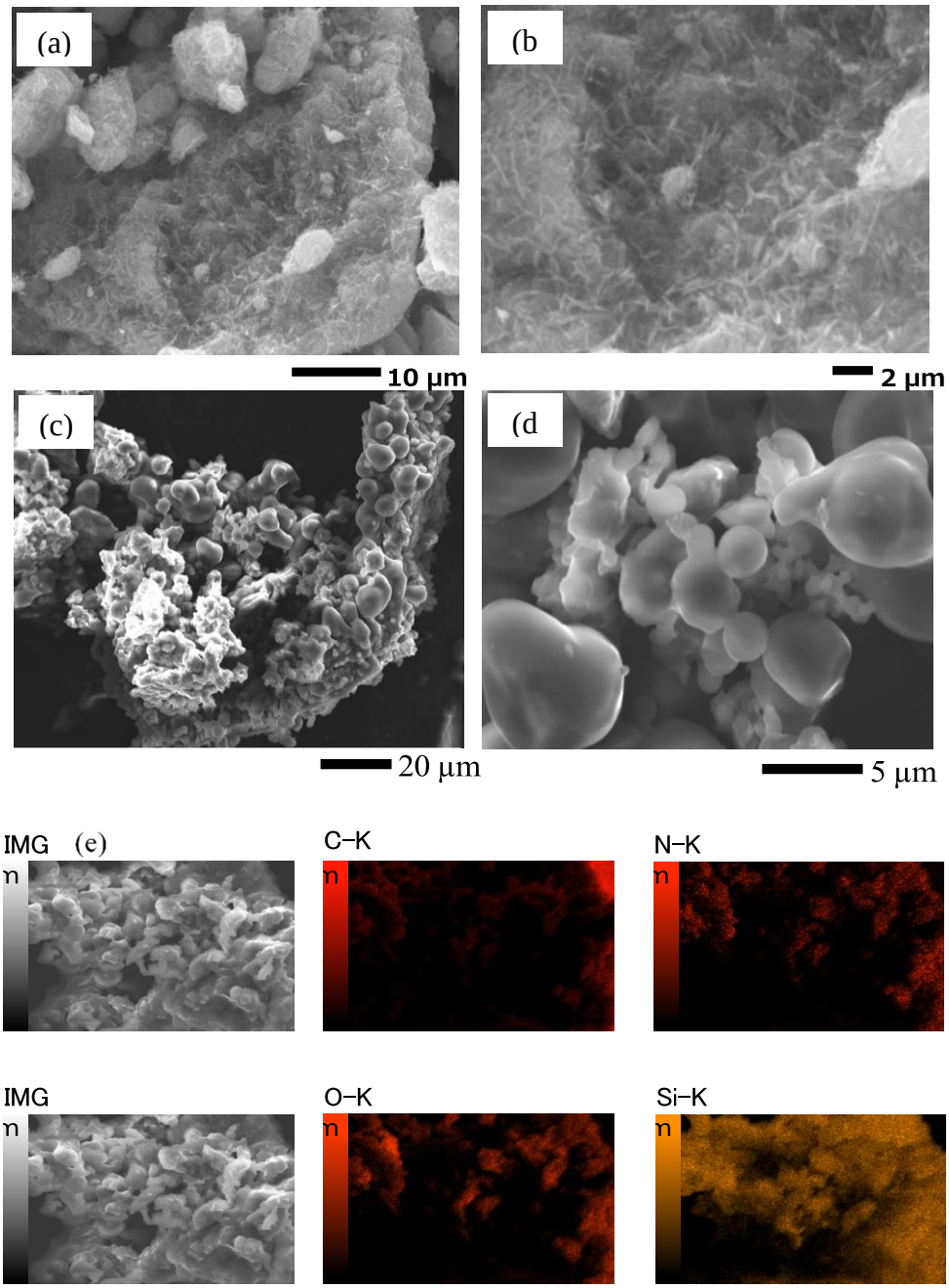

Figure 3. SEM images of (a, b) OMS-2 and (c, d) Amine-OMS-2; and EDX-mapping results for Amine-OMS-2 (e).

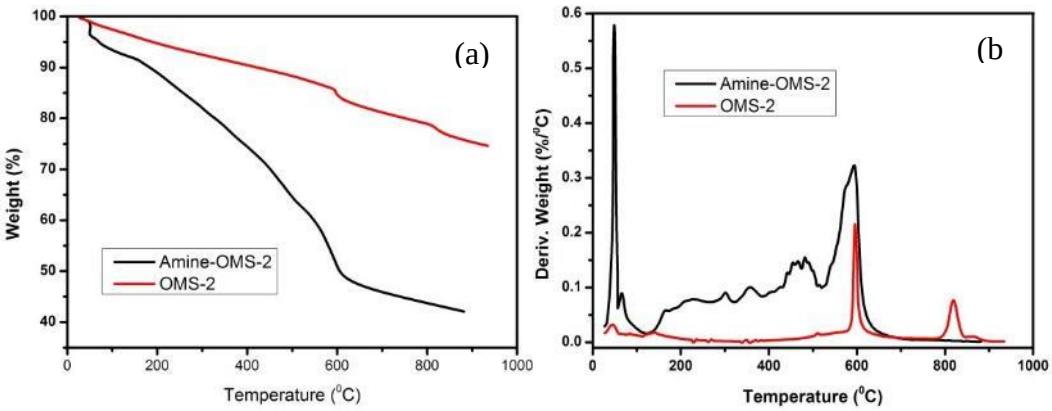

Figure 4. (a) TG and (b) DTG curves of Amine-OMS-2 and OMS-2.

Thermogravimetric analysis from 30 to 900 °C was performed to study the thermal stability of OMS-2 and Amine-OMS-2. Fig. 4 shows mass losses of 26 % for OMS-2 and 58 % for Amine-OMS-2. The low mass losses of 4 % for OMS-2 and 8 % for Amine-OMS-2 at 60-200 °C were from the evaporation of moisture or dehydration. At 600 °C, the masses of both OMS-2 and Amine-OMS-2 changed significantly, possibly due to the conversion of oxide in OMS-2 [40] and the degradation of amine in Amine-OMS-2 [23]. However, the Amine-OMS-2 sample displayed a large variation from 400 to 600 °C, corresponding to the combustion of organic compounds [41]. Comparison of the mass losses for OMS-2 and Amine-OMS-2 showed that the amount of amine accounted for about 40 % of the sample mass.

Adsorption of Nitrate and Phosphate

The nitrate and phosphate adsorption capacities fluctuated with solution pH (Fig. 5 (a)). The pH_{pzc} of the Amine-OMS-2 material was determined to be 4.7 (Fig. 5 (b)). When pH < pH_{pzc}, the positively charged surface electrostatically attracts both nitrate and phosphate anions. When pH > pH_{pzc}, the competition for surface sites by OH^- ions inhibits anion adsorption [42]. Here, the highest adsorption capacities were 34 mg g^{-1} at pH 5 for nitrate and 12 mg g^{-1} at pH 6 for phosphate. At pH values below 5, more H^+ ions are present, which hinders the adsorption of nitrate ions. In addition, there may be competitive adsorption of SO_4^{2-} from the pH adjustment process with H_2SO_4 solution [43]. At pH > 5, the decrease in nitrate adsorption is due to the competition between OH^- and nitrate ions [44]. In solution, phosphate dissociates into different forms of PO_4^{3-} (pH > 11), $H_2PO_4^-$ and HPO_4^{2-} (pH 7-11), and H_3PO_4 (pH 2-7) [43]. Under acidic conditions (pH < 7), the dominant form of $H_2PO_4^-$ easily interacts with amine groups in the adsorbent thanks to electrostatic interactions. This condition increases the phosphate adsorption capacity because the material carries a positive charge when pH < pH_{pzc} ~ 4.7. Although HPO_4^{2-} and PO_4^{3-} also exist at higher pH, the adsorption capacity is reduced due to competition from OH^- ions [45]. In summary, Amine-OMS-2 had the highest adsorption capacity for nitrate at pH 5 and for phosphate at pH 6, which is close to the pH value of real wastewater.

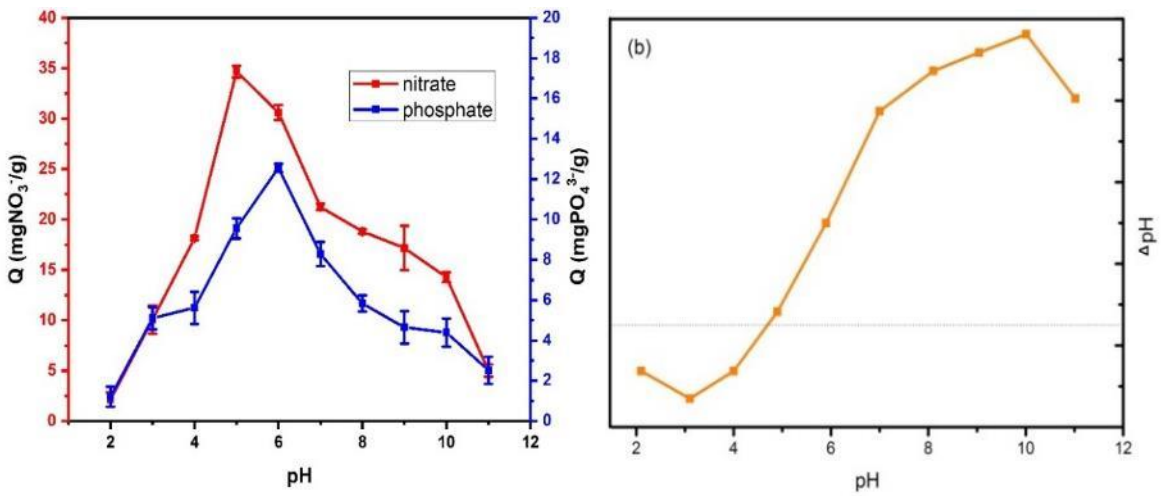

Figure 5. (a) Effects of initial solution pH on nitrate and phosphate adsorption, and (b) the isoelectric point of Amine-OMS-2.

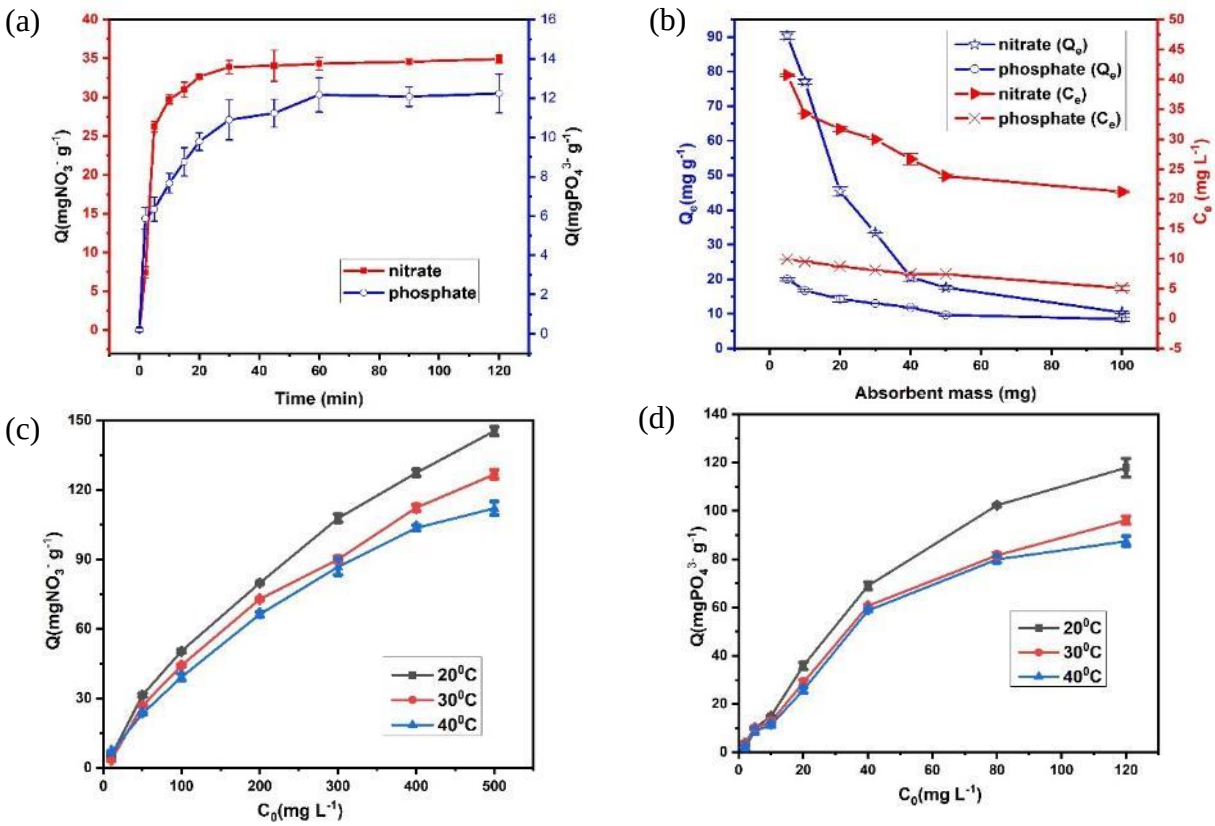

Figure 6. Adsorption capacities of nitrate and phosphate in relation to (a) time, (b) adsorbent mass, (c) initial concentration, and (d) temperature.

The nitrate and phosphate adsorption capacities of the materials increased with contact time (Fig. 6 (a)). In particular, the time to reach equilibrium for nitrate was faster than that for phosphate. The adsorption capacity increased rapidly to equilibrium condition after about 30 min for nitrate and 60 min for phosphate. The equilibrium time for nitrate was usually earlier than that for phosphate, and this is consistent with previous studies, as Amine-Chitosan materials have an equilibrium adsorption time of 30 min for nitrate and 45 min for phosphate [17]. With longer contact times, the adsorption capacities did not change significantly and reached stable levels of 34.06 mg g^{-1} (nitrate) and 12.17 mg g^{-1} (phosphate). The rapid adsorption equilibrium of Amine-OMS-2 is due to the strong interaction between the nitrate and phosphate anions and the amine groups. At a certain point, the anions attached to the surface become dense, signifying that the material is no longer able to capture more ions and becomes saturated [46, 47]. Since the amount of time to reach adsorption equilibrium was 30 min for nitrate and and 60 min for phosphate, an adsorption time of 60 min was chosen for subsequent experiments.

Three kinetic models of pseudo-first-order, pseudo-second-order, and intra-particle diffusion were then applied to the nitrate and phosphate adsorption reactions using Amine-OMS-2.

Pseudo-first-order kinetic model:

$$\ln (q_e - q_t) = \ln q_e - k_1 t \qquad \text{(Eq. 3)}$$

Pseudo-second-order kinetic model:

$$t/q_t = 1/(k_2 q_e^2) + t/q_e \qquad \text{(Eq. 4)}$$

Intra particle diffusion model:

$$q_t = k_p t^{1/2} + C \qquad \text{(Eq. 5)}$$

where k_1 (min^{-1}) and k_2 (g mg^{-1}/h^{-1}) are the apparent adsorption rate constants, k_p is the intra-particle diffusion rate constant (mg g^{-1} $h^{-1/2}$), C is the thickness of the boundary layer, and q_t and q_e are the amounts of ammonia adsorbed (mg g^{-1}) at time t (min) and at equilibrium, respectively.

The calculated kinetic parameters in Table 1 show that the pseudo-second-order model best describes the adsorption of nitrate and phosphate on Amine-OMS-2 because of its highest correlation coefficients (R^2) of 0.9978 for nitrate and 0.9973 for phosphate adsorption. Furthermore, its modelled adsorption capacities ($q_{e,\,cal}$) were 35.71 mg g^{-1} (nitrate) and 12.64 mg g^{-1} (phosphate), which were similar to the calculated experimental capacities ($q_{e,\,exp}$). Therefore, in this study, the nitrate and phosphate adsorption kinetics followed

the pseudo-second-order model, while the rate of adsorption was quadratic dependent on the capacity of Amine-OMS-2 [48].

Fig. 6 (b) shows that the adsorption capacity was greatly influenced by the mass of Amine-OMS-2. The nitrate and phosphate adsorption capacities were inversely proportional to the mass of the material, consistent with previous publications [19, 21, 23, 24]. The adsorption capacity is considered as milligrams of adsorbent per gram of adsorbent. As the adsorbent dosage increases, the contact area is higher when the nitrate and phosphate concentrations remain the same. Therefore, the adsorption capacity decreases when the mass of the adsorbent increases significantly. At the same time, as the mass of the material increases, the concentration of the adsorbed pollutant increases, leading to an increased treatment efficiency of the material.

Table 1. Correlation coefficients (R^2) and linear equations of kinetic models.

	Kinetic model	**Linear equation**	**R^2**	**Capacity ($q_{e,cal}$, mg g^{-1})**
Nitrate	Pseudo-first-order	y = -0.0233x + 1.7614	0.3413	5.82
	Pseudo-second-order	y = 0.028x + 0.0694	0.9978	35.71
	Intra-particle diffusion	y = 0.2793x + 2.4639	0.5927	-
Phosphate	Pseudo-first-order	y = -0.0293x + 1.5674	0.5279	4.79
	Pseudo-second-order	y = 0.0791x + 0.3394	0.9973	12.64
	Intra-particle diffusion	y = 0.2058x + 1.6052	0.9513	-

Table 2. The isotherm parameters of nitrate and phosphate adsorption.

Isotherm	**Parameter**	**Temperature (°C)**		
		20	30	40
Nitrate				
Langmuir	Q_{max} (mg g^{-1})	243.9	277.78	161.29
	K_L (L mg^{-1})	0.0038	0.0023	0.0053
	r^2	0.8973	0.6243	0.945
Freundlich	K_f ((mg g^{-1})(L mg^{-1})^n)	0.6568	1.1929	0.4707
	n	1.26	11.42	1.48
	r^2	**0.9625**	**0.9461**	**0.9982**
Phosphate				
Langmuir	Q_{max} (mg g^{-1})	208.33	151.52	175.44
	K_L (L mg^{-1})	0.3934	0.0057	0.0036
	r^2	0.7556	0.8153	0.7554
Freundlich	K_f ((mg g^{-1})(L mg^{-1})^n)	0.5779	0.5746	1.2934
	n	1.30	1.39	1.14
	r^2	**0.9667**	**0.9676**	**0.9665**

The output nitrate concentration was 27.10 mg L^{-1} at a material mass of 30 mg, which meets the requirement of Column A according to QCVN 14:2008/BTNMT (National technical regulations on domestic wastewater, where the allowable discharge concentrations of nitrate and phosphate are 30 and 6 mg L^{-1}, respectively). With phosphate, the output concentration was always lower than 6 mg L^{-1} in all tests. The adsorption capacity decreased rapidly with a material mass of < 30 mg but was not significant with a material mass of > 30 mg. Therefore, a material mass of 30 mg was selected for the subsequent experiments.

Fig. 6 (c) shows that the nitrate adsorption capacity was directly proportional to its initial concentration and inversely proportional to adsorption temperature. As the initial nitrate concentration increases, there are more of these ions in the solution, facilitating the interaction of these ions with the material, which promotes contact and anion capture of Amine-OMS-2. The nitrate ions become more mobile in solution as the temperature increases, resulting in their weaker capturing ability, which is clearly observed here at a nitrate concentration of ≥ 100 mg L^{-1} and temperature of 20-40 °C. Similar to nitrate, the phosphate adsorption capacity is also proportional to its initial concentration and inversely proportional to solution temperature (Fig. 6 (d)). The high density of phosphate ions promotes interactions at increasing solution concentrations; however, the increase in temperature hinders adsorption.

Langmuir and Freundlich isotherm models were employed to describe the correlation between nitrate and phosphate concentrations on the surface of Amine-OMS-2 with their concentrations in solution at equilibrium and constant temperature. The degree of agreement between theory and experiment is decided based on the correlation coefficient R^2 between the experimental values and the proposed model and the n factor in the Freundlich isotherm model ($1 < n < 10$ is favourable for the adsorption). As summarized in Table 2, adsorption isotherms followed the Freundlich model at all three temperatures, with correlation coefficients close to 1 for both nitrate and phosphate. Nitrate, had the highest R^2 of 0.9982 at 40 °C, showing that the Amine-OMS-2 surface had heterogeneity. At 30 °C, $n > 1$ indicates favourable adsorption [49]. The maximum adsorption capacities of nitrate and phosphate in water by Amine-OMS-2 were compared with those of other materials (Table 3), showing that only Amine-functionalized magnetic chitosan (AFMCS) composite beads were better than Amine-OMS-2 for nitrate adsorption, but Amine-OMS-2 was only better than carbon residue for phosphate adsorption. This may be due to the difference in the adsorption centres of the materials used, i.e., OMS-2 in our study and Fe_3O_4 in the AFMCS study. In the literature, Fe_3O_4 has been proven to be effective in adsorbing anions such as nitrate and phosphate [50].

In wastewater treatment, the adsorption system is usually installed at the tertiary treatment stage, after the major biological treatment processes. Adsorption is applied when the residual pollutant concentration in the wastewater is already low, a condition which is hard to treat by other methods. Therefore, to ascertain the feasibility of applying Amine-OMS-2 in practice, experiments with real wastewater samples after biological treatment were conducted. Amine-OMS-2 was able to remove nitrate and phosphate in wastewater with adsorption capacities of 11.07 and 16.78 mg g^{-1}, respectively. These values were not as high as those obtained with synthetic wastewater, which may be due to competitive adsorption by other anions present in real wastewater. In addition, Amine-OMS-2 was also capable of treating organic pollutants in wastewater, with a reduction in COD levels from 56.64 to 34.24 mg L^{-1}.

Table 3. Comparison with other materials in the literature.

Adsorbent	Nitrate (mg g^{-1})	Phosphate (mg g^{-1})	Reference
Amine-functionalized magnetic chitosan (AFMCS) composite beads	38.40	42.95	[15]
Ammonium-functionalized MCM-48	12.20	16.50	[51]
Carbon residue	30.20	11.20	[52]
$CuFe_2O_4$-2N-La	-	32.59	[53]
Amine functionalized bio-resin derived from corn stalk	6.48	48.73	[54]
Modified cocoa shell	31.65	-	[47]
Modified steel slag	6.16	-	[55]
Amine-OMS-2	34.06	12.17	This study

CONCLUSION

Amine-OMS-2 was successfully synthesized, characterized and applied to the removal of nitrate and phosphate in water. The equilibrium time and optimum pH were 30 min at pH 5 for nitrate and 60 min at pH 6 for phosphate. The kinetics of both the nitrate and phosphate adsorption reactions followed the pseudo-second-order model. Both nitrate and phosphate adsorption capacities increased with concentration but decreased with adsorbent mass. The nitrate and phosphate adsorption isotherms were also both consistent with the Freundlich model. Besides its ability to treat nitrate and phosphate, Amine-OMS-2 was also able to reduce COD levels in wastewater, which shows great potential for practical application.

REFERENCES

1. Bhatti, H. N., Hayat, J., Iqbal, M., Noreen, S. and Nawaz, S. (2018) Biocomposite application for the phosphate ions removal in aqueous medium. *Journal of Materials Research and Technology*, **7**, 300–307.

2. Gupta, S. K., Gupta, R., Gupta, A., Seth, A., Bassin, J. and Gupta, A. (2000) Recurrent acute respiratory tract infections in areas with high nitrate concentrations in drinking water. *Environmental health perspectives*, **108**, 363–366.

3. Majumdar, D. and Gupta, N. (2000) Nitrate pollution of groundwater and associated human health disorders. *Indian journal of environmental health*, **42**, 28–39.

4. Ward, M. H., DeKok, T. M., Levallois, P., Brender, J., Gulis, G., Nolan, B. T., et al. (2005) Workgroup report: drinking-water nitrate and health-recent findings and research needs. *Environmental health perspectives*, **113**, 1607–1614.

5. Rubio-Aliaga, I. (2020) Phosphate and kidney healthy aging. *Kidney Blood Pressure Research*, **45**, 1–10.

6. Abukhadra, M. R., Ali, S. M., Nasr, E. A., Mahmoud, H. A. A. and Awwad, E. M. (2020) Effective sequestration of phosphate and ammonium ions by the bentonite/zeolite Na–P composite as a simple technique to control the eutrophication phenomenon: realistic studies. *ACS omega*, **5**, 14656–14668.

7. Nandakumar, S., Pipil, H., Ray, S. and Haritash, A. J. C. (2019) Removal of phosphorous and nitrogen from wastewater in Brachiaria-based constructed wetland, **233**, 216–222.

8. Tran, L. B., Nguyen, T. T., Padungthon, S., Le, T. T., Nguyen Thi, Q. A. and Nguyen, N. H. J. N. C. W. (2022) Advanced natural hydrated iron-alum oxides cation exchange resin for simultaneous phosphate and hardness removal, **5**, 1–11.

9. Pirsaheb, M., Khosravi, T., Sharafi, K., Mouradi, M. J. D. and Treatment, W. (2016) Comparing operational cost and performance evaluation of electrodialysis and reverse osmosis systems in nitrate removal from drinking water in Golshahr. *Mashhad*, **57**, 5391–5397.

10. Huang, H., Liu, J., Zhang, P., Zhang, D. and Gao, F. J. C. E. J. (2017) Investigation on the simultaneous removal of fluoride, ammonia nitrogen and phosphate from semiconductor wastewater using chemical precipitation, **307**, 696–706.

11. Lee, K. -C. and Rittmann, B. E. J. W. R. (2003) Effects of pH and precipitation on autohydrogenotrophic denitrification using the hollow-fiber membrane-biofilm reactor, **37**, 1551–1556.

12. Gao, Q., Wang, C. -Z., Liu, S., Hanigan, D., Liu, S. -T. and Zhao, H. -Z. J. C. E. J. (2019) Ultrafiltration membrane microreactor (MMR) for simultaneous removal of nitrate and phosphate from water, **355**, 238–246.

13. Dongre, R. S. J. R. and Science, D. I. M. (2018) Phosphate & Nitrate Removal from Agricultural Runoff by Chitosan-Graphite Composite, **11**.

14. Mulkerrins, D., Dobson, A. and Colleran, E. (2004) Parameters affecting biological phosphate removal from wastewaters. *Environment International*, **30**, 249–259.

15. Aswin Kumar, I. and Viswanathan, N. (2018) Development and reuse of amine-grafted chitosan hybrid beads in the retention of nitrate and phosphate. *Journal of Chemical & Engineering Data*, **63**, 147–158.

16. Zhang, M., Gao, B., Yao, Y., Xue, Y. and Inyang, M. (2012) Synthesis of porous MgO-biochar nanocomposites for removal of phosphate and nitrate from aqueous solutions. *Chemical Engineering Journal*, **210**, 26–32.

17. Sowmya, A. and Meenakshi, S. (2013) An efficient and regenerable quaternary amine modified chitosan beads for the removal of nitrate and phosphate anions. *Journal of Environmental Chemical Engineering*, **1**, 906–915.

18. Toan, P. P., Thanh, N. T. and Huy, N. N. (2019) Characterization and adsorption capacity of amine-SiO2 material for nitrate and phosphate removal. *Vietnam Journal of Science and Technology*, **57**, 492.

19. Phan, P. T., Nguyen, T. T., Nguyen, N. H. and Padungthon, S. (2019) A simple method for

synthesis of triamine-SiO_2 material toward aqueous nitrate adsorption. *Environment and Natural Resources Journal*, **17**, 59–67.

20. Thanh, N. T., Huy, N. N., Minh, T. V. and Toan, P. P. (2019) Characterization and phosphate adsorption capacity of anion exchange resin-supported iron hydroxide material. *AGU International Journal of Sciences*, **7**, 82–90.

21. Phan, P. T., Nguyen, T. A., Nguyen, N. H. and Nguyen, T. T. (2020) Modelling approach to nitrate adsorption on triamine-bearing activated rice husk ash. *Engineering and Applied Science Research*, **47**, 190–197.

22. Phan, P. T., Nguyen, T. T., Nguyen, N. H. and Padungthon, S. (2019) Triamine-bearing activated rice husk ash as an advanced functional material for nitrate removal from aqueous solution. *Water Science and Technology*, **79**, 850–856.

23. Nguyen, T. T., Le, T. T., Phan, P. T. and Nguyen, N. H. (2020) Preparation, Characterization, and Application of Novel Ferric Oxide-Amine Material for Removal of Nitrate and Phosphate in Water. *Journal of Chemistry*, **2020**, 8583543.

24. Nguyen, T. T., Tran, V. A. K., Tran, L. B., Phan, P. T., Nguyen, M. T., Bach, L. G., et al. (2021) Synthesis of cation exchange resin-supported iron and magnesium oxides/hydroxides composite for nitrate removal in water. *Chinese Journal of Chemical Engineering*, **32**, 378–384.

25. Phuoc Toan, P., Nguyen, T. T., Le, T. T., Le, N. H., Padungthon, S. and Nguyen, N. H. (2021) Synthesis of flower-like iron oxide/hydroxide on rice husk ash support and its application for phosphate removal in water. *Journal of Water Chemistry and Technology*, **43**, 108–115.

26. Randall, S. R., Sherman, D. M. and Ragnarsdottir, K. V. (1998) An extended X-ray absorption fine structure spectroscopy investigation of cadmium sorption on cryptomelane (KMn8O16). *Chemical geology*, **151**, 95–106.

27. Nguyen, N. H., Nguyen Thi, B. T., Nguyen Le, T. G., Nguyen Thi, Q. A., Phan, P. T., Bach, L. G., et al. (2020) Enhancing the activity and stability of CuO/OMS-2 catalyst for CO oxidation at low temperature by modification with metal oxides. *International Journal of Chemical Engineering*, **2020**, 8827995.

28. Thao, N. T. B. and Huy, N. N. (2019) Thermal oxidation of carbon monoxide in air using various self-prepared catalysts. *Science & Technology Development Journal-Engineering and Technology*, **2**, SI31–SI39.

29. Anh, N. T. Q. and Thanh, N. T. (2018) Binary copper and manganese oxide nanoparticle supported OMS-2 for enhancing activity and stability toward CO oxidation reaction at low temperature. *Vietnam Journal of Science and Technology*, **56**, 741.

30. Kosmulski, M. (2006) pH-dependent surface charging and points of zero charge: III. Update. *Journal of colloid interface science*, **298**, 730–741.

31. Garces, L., Hincapie, B., Makwana, V., Laubernds, K., Sacco, A. and Suib, S. (2003) Effect of using polyvinyl alcohol and polyvinyl pyrrolidone in the synthesis of octahedral molecular sieves. *Microporous and mesoporous materials*, **63**, 11–20.

32. Abulizi, A., Yang, G. H., Okitsu, K. and Zhu, J. -J. (2014) Synthesis of MnO2 nanoparticles from sonochemical reduction of MnO4− in water under different pH conditions. *Ultrasonics sonochemistry*, **21**, 1629–1634.

33. Julien, C., Massot, M., Poinsignon, C. J. S. A. P. A. M. and Spectroscopy, B. (2004) Lattice vibrations of manganese oxides: Part I. Periodic structures, **60**, 689–700.

34. Liu, X. -S., Jin, Z. -N., Lu, J. -Q., Wang, X. -X. and Luo, M. -F. (2010) Highly active CuO/OMS-2 catalysts for low-temperature CO oxidation. *Chemical Engineering Journal*, **162**, 151–157.

35. Nui, P. X., Son, L. V. and Thi, T. T. V. (2016) Synthesis and Characterization of (3-aminopropyl) Triethoxysilane Coated Magnetite Nanoparticles for Drug Delivery. *VNU Journal of Science: Natural Sciences and Technology*, **32**, 143–150.

36. Phan, P. T., Nguyen, T. T., Nguyen, N. H. and Padungthon, S. J. W. S., Technology (2019) Triamine-bearing activated rice husk ash as an advanced functional material for nitrate removal from aqueous solution, **79**, 850–856.

37. Song, H., Zhou, Y., Li, A. and Mueller, S. (2012) Selective removal of nitrate from water by a macroporous strong basic anion exchange resin. *Desalination*, **296**, 53–60.

38. Abou Taleb, M. F., Mahmoud, G. A., Elsigeny, S. M. and Hegazy, E. -S. A. (2008) Adsorption and desorption of phosphate and nitrate ions using quaternary (polypropylene-g-N,N-dimethyl-amino ethylmethacrylate) graft copolymer. *Journal of Hazardous Materials*, **159**, 372–379.

39. King'ondu, C. K., Opembe, N., Chen, C. H., Ngala, K., Huang, H., Iyer, A., et al. (2011) Manganese oxide octahedral molecular sieves (OMS-2) multiple framework substitutions: A

new route to OMS-2 particle size and morphology control, **21**, 312–323.

40. Said, S., Riad, M., Helmy, M., Mikhail, S., Khalil, L. J. C. and Research, M. (2014) Effect of the different preparation methods on the characterization and the catalytic activity of the nano-structured cryptomelane materials, **6**, 27–41.

41. Chen, Y. -H. and Lu, D. -L. (2014) Amine modification on kaolinites to enhance CO2 adsorption. *Journal of colloid interface science*, **436**, 47–51.

42. Bravo, A., Garcia, J., Domenech, X. and Peral, J. (1993) Some aspects of the photocatalytic oxidation of ammonium ion by titanium dioxide. *Journal of chemical research. Synopses (Print)*, 376–377.

43. Zhang, Q., Zhang, Z., Teng, J., Huang, H., Peng, Q., Jiao, T., et al. (2015) Highly efficient phosphate sequestration in aqueous solutions using nano-magnesium hydroxide modified polystyrene materials. *Industrial & Engineering Chemistry Research*, **54**, 2940–2949.

44. Yan, L. -G., Yang, K., Shan, R. -R., Yan, T., Wei, J., Yu, S. -J., et al. (2015) Kinetic, isotherm and thermodynamic investigations of phosphate adsorption onto core–shell Fe_3O_4@ LDHs composites with easy magnetic separation assistance. *Journal of Colloid and Interface Science*, **448**, 508–516.

45. Ngah, W. W., Teong, L. and Hanafiah, M. M. (2011) Adsorption of dyes and heavy metal ions by chitosan composites: A review. *Carbohydrate polymers*, **83**, 1446–1456.

46. Rajeswari, A., Amalraj, A. and Pius, A. (2016) Adsorption studies for the removal of nitrate using chitosan/PEG and chitosan/PVA polymer composites. *Journal of Water Process Engineering*, **9**, 123–134.

47. Fotsing, P. N., Bouazizi, N., Woumfo, E. D., Mofaddel, N., Le Derf, F. and Vieillard, J. (2021) Investigation of chromate and nitrate removal by adsorption at the surface of an amine-modified cocoa shell adsorbent. *Journal of Environmental Chemical Engineering*, **9**, 104618.

48. Ho, Y. -S. and Ofomaja, A. E. (2006) Pseudo-second-order model for lead ion sorption from aqueous solutions onto palm kernel fiber. *Journal of Hazardous Materials*, **129**, 137–142.

49. Chabani, M., Amrane, A. and Bensmaili, A. (2006) Kinetic modelling of the adsorption of nitrates by ion exchange resin. *Chemical Engineering Journal*, **125**, 111–117.

50. Katal, R., Pourkarimi, S., Bahmani, E., Dehkordi, H. A., Ghayyem, M. A., Esfandian, H. J. J. O. V., et al. (2013) Synthesis of Fe3O4/polyaniline nanocomposite and its application for nitrate removal from aqueous solutions, **19**, 147–156.

51. Saad, R., Belkacemi, K. and Hamoudi, S. (2007) Adsorption of phosphate and nitrate anions on ammonium-functionalized MCM-48: effects of experimental conditions. *Journal of colloid interface science*, **311**, 375–381.

52. Kilpimaa, S., Runtti, H., Kangas, T., Lassi, U. and Kuokkanen, T. (2015) Physical activation of carbon residue from biomass gasification: Novel sorbent for the removal of phosphates and nitrates from aqueous solution. *Journal of Industrial Engineering Chemistry*, **21**, 1354–1364.

53. Gu, W., Li, X., Xing, M., Fang, W. and Wu, D. (2018) Removal of phosphate from water by amine-functionalized copper ferrite chelated with La (III). *Science of the Total Environment*, **619**, 42–48.

54. Pan, J., Gao, B., Song, W., Xu, X., Jin, B. and Yue, Q. (2019) Column adsorption and regeneration study of magnetic biopolymer resin for perchlorate removal in presence of nitrate and phosphate. *Journal of Cleaner Production*, **213**, 762–775.

55. Yang, L., Yang, M., Xu, P., Zhao, X., Bai, H. and Li, H. (2017) Characteristics of nitrate removal from aqueous solution by modified steel slag. *Water*, **9**, 757.